processes

MDPI

Article

Thermodynamic Analysis of Hydrogen Production from Bio-Oil Steam Reforming Utilizing Waste Heat of Steel Slag

Zhijun Ding [1], Yang Liu [2], Xin Yao [1,*], Yuekai Xue [1,*], Chenxiao Li [1,*], Zhihui Li [1], Shuhuan Wang [1] and Jianwei Wu [3]

[1] College of Metallurgy and Energy, North China University of Science and Technology, Tangshan 063210, China; sgdingzhijun@hbisco.com (Z.D.); lzh@ncst.edu.cn (Z.L.); wshh88@ncst.edu.cn (S.W.)
[2] Health Center, North China University of Science and Technology, Tangshan 063210, China; liuyangineur@outlook.com
[3] School of Metallurgy, Northeastern University, Shenyang 110819, China; wujianweiup@163.com
* Correspondence: yaoxin_0129@163.com (X.Y.); xueyuekai965@163.com (Y.X.); lichenxiao34@163.com (C.L.)

Abstract: (1) Background: The discharged temperature of steel slag is up to 1450 °C, representing heat having a high calorific value. (2) Motivation: A novel technology, integrating bio-oil steam reforming with waste heat recovery from steel slag for hydrogen production, is proposed, and it is demonstrated to be an outstanding method via thermodynamic calculation. (3) Methods: The equilibrium productions of bio-oil steam reforming in steel slag under different temperatures and S/C ratios (the mole ratio of steam to carbon) are obtained by the method of minimizing the Gibbs free energy using HSC 6.0. (4) Conclusions: The hydrogen yield increases first and then decreases with the increasing temperature, but it increases with the increasing S/C. Considering equilibrium calculation and actual application, the optimal temperature and S/C are 706 °C and 6, respectively. The hydrogen yield and hydrogen component are 109.13 mol/kg and 70.21%, respectively, and the carbon yield is only 0.08 mol/kg under optimal conditions. Compared with CaO in steel slag, iron oxides have less effect on hydrogen production from bio-oil steam reforming in steel slag. The higher the basicity of steel slag, the higher the obtained hydrogen yield and hydrogen component of bio-oil steam reforming in steel slag. It is demonstrated that appropriately decreasing iron oxides and increasing basicity could promote the hydrogen yield and hydrogen component of bio-oil steam reforming that utilizes steel slag as a heat carrier during the industrial application.

Keywords: thermodynamic analysis; heat recovery; steam reforming; bio-oil; steel slag

Citation: Ding, Z.; Liu, Y.; Yao, X.; Xue, Y.; Li, C.; Li, Z.; Wang, S.; Wu, J. Thermodynamic Analysis of Hydrogen Production from Bio-Oil Steam Reforming Utilizing Waste Heat of Steel Slag. *Processes* **2023**, *11*, 2342. https://doi.org/10.3390/pr11082342

Academic Editor: Shetian Liu

Received: 30 June 2023
Revised: 21 July 2023
Accepted: 27 July 2023
Published: 3 August 2023

1. Introduction

The goal of a dual-carbon strategy was proposed via China in 2020, which is that the CO_2 emissions reach a peak in 2030 and are neutral in 2060. Steel enterprises are a national pillar of life and production, but have high energy consumption and high carbon dioxide emissions [1,2]. The development of green metallurgy technology could provide a solid foundation for the dual-carbon strategy. Statistics indicates that China is the largest crude steel producer in the world, with production of 1032.8 million tons [3]. The energy consumption of steel enterprises in China is about 23% of the total consumption [4]. However, 70% of the energy used in steel enterprises is discharged as waste heat and waste energy [5,6]. Reasonable recovery of waste heat and waste energy is an effective method for the green metallurgy process. Steelmaking is the primary process of steel enterprises and consumes a huge amount of energy. Steel slag is a by-product of the steelmaking process, and has a discharge temperature of up to 1450 °C, representing heat having a high calorific value [7–9]. However, steel slag is disposed of via the water quenching method in the actual production process. The high calorific value of steel slag is not recovered reasonably. Thus, the recovery of waste heat from steel slag could become a key technology to recover waste heat and waste energy during the steel production process.

The methods of recovering waste heat from slag include physical methods and chemical methods. The physical methods use the waste heat of steel slag to heat water or cool College of Metallurgy and Energy, air. The chemical methods use chemical reactions to replace the waste heat of steel slag. Li investigated the thermodynamic analysis of the physical and chemical methods used to recover waste heat from slag via the enthalpy–exergy compass [10]. The results implied that the heat efficiency and exergy efficiency of physical methods were 76.9% and 34.2%, respectively, but the heat efficiency and exergy efficiency of chemical methods increased to 92.2% and 60%, respectively. Compared to physical methods, chemical methods can recover waste heat from slag with a high reaction rate and high efficiency [11–13]. Using chemical reactions to recover waste heat from slag was proposed and has been investigated from the perspectives of thermodynamics, dynamics, product characterization, etc. Kasai first proposed using steam reforming of methane recovery of waste heat from blast furnace slag [14]. The results implied that steam reforming of methane could efficiently recover waste heat from blast furnace slag. The feasibilities of coal gasification [15,16], biomass gasification [8], and bio-oil steam reforming [17] to recover waste heat from blast furnace slag were demonstrated via thermodynamic calculations. These chemical reactions could efficiently replace the waste heat of blast furnace slag. The dynamic characterizations of coal gasification [18,19], biomass gasification [13,20], and sludge gasification [21,22] in blast furnace slag were investigated via dynamic calculations. The results implied that blast furnace slag could decrease the reaction activation energy, and was thus regarded as an outstanding heat carrier. The product characterizations of biogas [23], municipal solid waste gasification [24], coal gasification [25,26], and sludge pyrolysis [27,28] using blast furnace slag as a heat carrier were investigated. The results implied that blast furnace slag could weaken the C-C bond, which catalyzed the process of using chemical reactions to recover waste heat from blast furnace slag. The waste heat of blast furnace slag could be efficiently replaced via chemical reactions and these chemical reactions could provide energy for the steel production process. This was a foundation for green metallurgy development.

Meanwhile, with the depletion of fossil fuels, renewable energy has gradually been explored by researchers. Hydrogen is regarded as a green energy resource for metallurgy industrial applications [29,30], and it can be obtained via petroleum cracking, coal pyrolysis, natural gas reforming, oil reforming, biomass pyrolysis, biomass gasification, etc. [31]. Biomass pyrolysis and gasification applications are outstanding methods used to obtain hydrogen. However, during the process of biomass pyrolysis and gasification, bio-oil can be obtained, decreasing the utilization efficiency of biomass. Utilization of bio-oil reforming has been proven to be a feasible and efficient method to increase the utilization efficiency of biomass and obtain hydrogen [32–34]. The reaction rate and heat source of bio-oil steam reforming are the main factors that limit the technological progress. In order to obtain hydrogen efficiently, studies have investigated the characterizations of the bio-oil steam reforming process over catalysts and obtained the catalyst property of the reforming process [32,33]. In order to identify a proper heat source for bio-oil reforming, our team proposed using reforming of bio-oil recovery of waste heat from blast furnace slag [17,35,36]. The results implied that CaO in blast furnace slag was the basic component for catalyzing the steam reforming process.

In a review of recovering waste heat from slag, researchers have primarily focused on recovering waste heat from blast furnace slag. Results showed that the higher the ratio of CaO to SiO_2, the higher the rate of the obtained methane–steam reaction [37]. The ratio of CaO to SiO_2 in steel slag is higher than that in blast furnace slag [8]. However, the characterizations of steam reforming of bio-oil in steel slag are ambiguous, and are first proposed in this paper. Temperature and steam are the main factors affecting the process of steam reforming of bio-oil. In addition, the components of steel slag vary enormously during the production processes. The effects of temperature, S/C, and type of steel slag on the equilibrium productions of steam reforming of bio-oil are explored via thermodynamic calculations in this paper, and the optimal condition is obtained. This can provide a

theoretical foundation for the recovery of waste heat from steel slag during the process of metallurgy industrial application in the future.

2. Methodology

2.1. Materials

To obtain the thermodynamic characterizations of bio-oil steam reforming using steel slag as a heat carrier, the chemical compositions of bio-oil and steel slag should be determined. The bio-oil is complicated, but it mainly contains alcohols, acids, ketones, and phenols. In addition, the equal mass ratio of acetic acid, ethanol, acetone, and phenol can be used as the bio-oil model compound during the process of bio-oil reforming, as demonstrated in our previous studies [17,35]. The equal mass ratio of acetic acid, ethanol, acetone, and phenol is also used to replace bio-oil in the paper. In addition, the mass ratio of steel slag to bio-oil is 1:1 and the bio-oil is also defined as 1 kg during the process of thermodynamic calculations The contents of FeO and Fe_2O_3 in steel slag and the basicity of steel slag may affect the equilibrium production of bio-oil steam reforming using steel slag as a heat carrier. Steel slag with different quantities of FeO and Fe_2O_3 and levels of basicity is used in the thermodynamic calculation and their characterizations are shown in Table 1.

Table 1. The compositions of steel slag.

Type of Steel Slag	CaO	SiO_2	Al_2O_3	MgO	Fe_2O_3	FeO	Fe_2O_3 + FeO	R
1	54.00	18.00	8.00	5.00	4.75	10.25	15.00	3
2	50.25	16.75	8.00	5.00	6.33	13.67	20.00	3
3	46.50	15.50	8.00	5.00	7.92	17.08	25.00	3
4	42.75	14.25	8.00	5.00	9.50	20.50	30.00	3
5	39.00	13.00	8.00	5.00	11.08	23.92	35.00	3
6	41.33	20.67	8.00	5.00	7.92	17.08	25.00	2
7	44.29	17.71	8.00	5.00	7.92	17.08	25.00	2.5
8	46.50	15.50	8.00	5.00	7.92	17.08	25.00	3
9	48.22	13.78	8.00	5.00	7.92	17.08	25.00	3.5
10	49.60	12.40	8.00	5.00	7.92	17.08	25.00	4

R is basicity, which is the mass ratio of CaO to SiO_2.

2.2. Thermodynamic Method

The chemical reaction of steam reforming of the bio-oil recovery of waste heat from steel slag contains complex mechanisms. When using the minimization of Gibbs free energy method, mastering the possible reactant production can only be used to obtain equilibrium productions. The minimization of Gibbs free energy has been proven to efficiently yield the equilibrium production and was applied in our previous studies [17,38]. The HSC 6.0 software with the function of the minimization of Gibbs free energy is also used in this paper. The thermodynamic characterizations of bio-oil steam reforming in blast furnace slag were investigated in our previous study [17]. The oxide species in steel slag are consistent with those of blast furnace slag. Thus, the possible reactant productions of bio-oil steam reforming in steel slag are consistent with those in blast furnace slag. The principle of minimization of Gibbs free energy in HSC 6.0 software, and the possible reactant production of bio-oil steam reforming in steel slag, are described in our previous study [17]. The primary reactions in the process of the steam reforming of the bio-oil recovery of waste heat from steel slag are shown as follows:

Thermal cracking reaction (TCR):

$$C_nH_mO_k \rightarrow C_xH_yO_z + oH_2 + pCO + qCO_2 + rCH_4 + sC,\ \Delta H^{\theta}_{800^{\circ}C} > 0 \quad (1)$$

Steam reforming reactions (SRRs):

$$C_2H_6O + 3H_2O \rightarrow 2CO_2 + 6H_2,\ \Delta H^{\theta}_{800^{\circ}C} = 210.26\ \text{kJ mol}^{-1} \quad (2)$$

$$C_2H_4O_2 + 2H_2O \rightarrow 2CO_2 + 4H_2,\ \Delta H^{\theta}_{800^{\circ}C} = 153.33\ \text{kJ mol}^{-1} \quad (3)$$

$$C_3H_6O + 5H_2O \rightarrow 3CO_2 + 8H_2,\ \Delta H^{\theta}_{800^{\circ}C} = 295.90\ \text{kJ mol}^{-1} \quad (4)$$

$$C_6H_6O + 11H_2O \rightarrow 6CO_2 + 14H_2,\ \Delta H^{\theta}_{800^{\circ}C} = 473.68\ \text{kJ mol}^{-1} \quad (5)$$

$$C_xH_yO_z + (2x - z)H_2O \rightarrow xCO_2 + (2x + y/2 - z)H_2,\ \Delta H^{\theta}_{800^{\circ}C} > 0 \quad (6)$$

$$CH_4 + 2H_2O \rightarrow CO_2 + 4H_2,\ \Delta H^{\theta}_{800^{\circ}C} = 191.10\ \text{kJ mol}^{-1} \quad (7)$$

Methanation reactions (MRs):

$$CO + 3H_2 \rightarrow CH_4 + H_2O,\ \Delta H^{\theta}_{800^{\circ}C} = -225.22\ \text{kJ mol}^{-1} \quad (8)$$

$$C + 2H_2 \rightarrow CH_4,\ \Delta H^{\theta}_{800^{\circ}C} = -89.45\ \text{kJ mol}^{-1} \quad (9)$$

Water gas reaction (WGR):

$$C + H_2O \rightarrow CO + H_2,\ \Delta H^{\theta}_{800^{\circ}C} = 135.77\ \text{kJ mol}^{-1} \quad (10)$$

Water gas shift reaction (WGSR):

$$CO + H_2O \rightarrow H_2 + CO_2,\ \Delta H^{\theta}_{800^{\circ}C} = -34.12\ \text{kJ mol}^{-1} \quad (11)$$

Bell reaction (BR):

$$2CO \rightarrow C + CO_2,\ \Delta H^{\theta}_{800^{\circ}C} = -169.88\ \text{kJ mol}^{-1} \quad (12)$$

Reactions of mineral oxides with the generated gases (RMGs):

$$CaO + CO_2 \rightarrow CaCO_3,\ \Delta H^{\theta}_{800^{\circ}C} = -167.62\ \text{kJ mol}^{-1} \quad (13)$$

$$CaO + H_2O \rightarrow Ca(OH)_2,\ \Delta H^{\theta}_{800^{\circ}C} = -61.88\ \text{kJ mol}^{-1} \quad (14)$$

$$Fe_2O_3 + H_2 \rightarrow 2FeO + H_2O,\ \Delta H^{\theta}_{800^{\circ}C} = 28.89\ \text{kJ mol}^{-1} \quad (15)$$

$$Fe_2O_3 + CO \rightarrow 2FeO + CO_2,\ \Delta H^{\theta}_{800^{\circ}C} = -5.23\ \text{kJ mol}^{-1} \quad (16)$$

$$4Fe_2O_3 + CH_4 \rightarrow 8FeO + CO_2 + 2H_2O,\ \Delta H^{\theta}_{800^{\circ}C} = 306.64\ \text{kJ mol}^{-1} \quad (17)$$

$$1.132Fe_2O_3 + H_2 \rightarrow 2.395Fe_{0.945}O + H_2O,\ \Delta H^{\theta}_{800^{\circ}C} = 40.95\ \text{kJ mol}^{-1} \quad (18)$$

$$1.132Fe_2O_3 + CO \rightarrow 2.395Fe_{0.945}O + CO_2,\ \Delta H^{\theta}_{800^{\circ}C} = 6.84\ \text{kJ mol}^{-1} \quad (19)$$

$$4.527Fe_2O_3 + CH_4 \rightarrow 9.581Fe_{0.945}O + CO_2 + 2H_2O,\ \Delta H^{\theta}_{800^{\circ}C} = 353.98\ \text{kJ mol}^{-1} \quad (20)$$

$$Fe_2O_3 + 3H_2 \rightarrow 2Fe + 3H_2O,\ \Delta H^{\theta}_{800^{\circ}C} = 63.356\ \text{kJ mol}^{-1} \quad (21)$$

$$Fe_2O_3 + 3CO \rightarrow 2Fe + 3CO_2, \Delta H^{\theta}_{800^{\circ}C} = -38.99 \text{ kJ mol}^{-1} \quad (22)$$

$$1.333Fe_2O_3 + CH_4 \rightarrow 2.667Fe + CO_2 + 2H_2O, \Delta H^{\theta}_{800^{\circ}C} = 275.35 \text{ kJ mol}^{-1} \quad (23)$$

$$FeO + H_2 \rightarrow Fe + H_2O, \Delta H^{\theta}_{800^{\circ}C} = 17.24 \text{ kJ mol}^{-1} \quad (24)$$

$$FeO + CO \rightarrow Fe + CO_2, \Delta H^{\theta}_{800^{\circ}C} = -16.88 \text{ kJ mol}^{-1} \quad (25)$$

$$4FeO + CH_4 \rightarrow 4Fe + CO_2 + 2H_2O, \Delta H^{\theta}_{800^{\circ}C} = 260.04 \text{ kJ mol}^{-1} \quad (26)$$

2.3. Performance Evaluation

Gas yield and dry gas concentration are used to evaluate the performance of the process of steam reforming of the bio-oil recovery of waste heat from steel slag. The gas yield encompasses the H_2 yield, CO yield, and CH_4 yield. The dry gas concentration includes the H_2 concentration, CO concentration, and CH_4 concentration. The explanations of gas yield and dry gas concentration are shown as follows:

$$\text{Gas yield} = \frac{\text{The mole of production of bio} - \text{oil steam reforming}}{\text{The quality of bio} - \text{oil}} (\text{mol/kg}) \quad (27)$$

$$\text{Dry gas concentration} = \frac{\text{The mole of production in dry reforming gas}}{\text{The totalmole of dry reforming gas}} (\%) \quad (28)$$

The effects of conditions (temperature, S/C (the mole ratio of steam to the carbon in bio-oil), basicity, and iron oxide) on the process of steam reforming of the bio-oil recovery of waste heat from steel slag were obtained via PY and DGC. Subsequently, the mechanism of steam reforming of the bio-oil recovery of waste heat from steel slag was obtained.

3. Results and Discussion

3.1. Effect of Temperature

The process of steam reforming of the bio-oil recovery of waste heat from steel slag contains endothermic reactions and exothermic reactions. The temperature can affect the coupling endothermic reactions and exothermic reactions, further affecting the equilibrium product distribution [39,40]. The effects of temperature on the PY and DGC of steam reforming of the bio-oil recovery of waste heat from steel slag are illustrated in this section.

Taking the characterizations of steel slag-3 as an example, the hydrogen yields under different temperatures and S/C ratios are shown in Figure 1. Figure 1 shows that hydrogen production from bio-oil steam reforming in steel slag is feasible, and the hydrogen yield first increases then decreases with increasing temperature. Taking S/C of 6 as an example, the hydrogen yield increases from 0.90 mol/kg to 90.42 mol/kg as the temperature increases from 200 °C to 739 °C. Then, hydrogen yield decreases from 90.42 mol/kg to 84.94 mol/kg as the temperature increases from 739 °C to 1000 °C. At low temperatures, the endothermic reactions of TCR (Equation (1)), SRR (Equations (2)–(7)), and WGR (Equation (10)), and the exothermal reactions of MR (Equations (8) and (9)), are the main factors that affect the hydrogen yield. With the increase in temperature, TCR (Equation (1)), SRR (Equations (2)–(7)), and WGR (Equation (10)) shift to the right, and MR (Equation (8)) shifts to the left, and the hydrogen yield increases. However, at high temperatures, the exothermal reaction of WGSR (Equation (11)) is the main factor that affects the hydrogen yield. With the increase in temperature, WGSR (Equation (11)) shifts to the left, decreasing the hydrogen yield. Xie [40] and Yao [17] also investigated the characterizations of hydrogen production from the process of bio-oil steam reforming in blast furnace slag, and a similar variation in

hydrogen yield was obtained. They provide further evidence that the results of this paper are accurate.

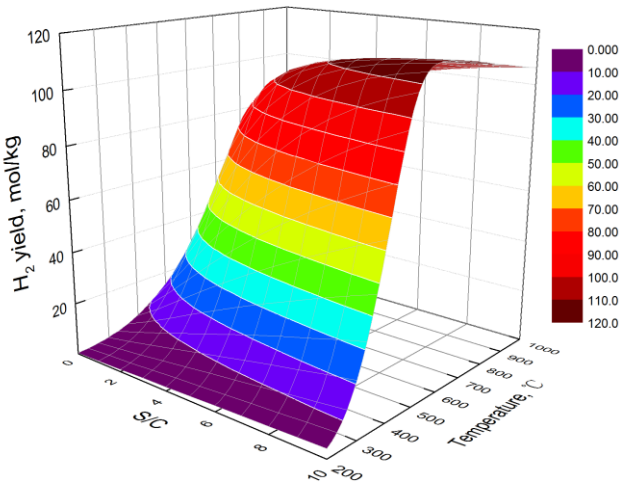

Figure 1. Hydrogen yields under different temperatures and S/C ratios.

Taking the characterizations of steel slag-3 as an example, the carbon monoxide yields under different temperatures and S/C ratios are illustrated in Figure 2. In Figure 2, the carbon monoxide yields increase with the increase in temperature. Taking S/C of 5 as an example, the carbon monoxide yield increases from 0.00 mol/kg to 22.49 mol/kg when the temperature increases from 200 °C to 1000 °C. The endothermic reactions of TCR (Equation (1)) and WGR (Equation (10)), and the exothermal reactions of MR (Equation (8)), WGSR (Equation (11)), BR (Equation (12)), and RMG (Equations (16), (22) and (25)), are the main factors that affect the carbon monoxide yield. With the increasing temperature, the endothermic reactions of TCR (Equation (1)) and WGR (Equation (10)) shift to the right, and the exothermal reactions of MR (Equation (8)), WGSR (Equation (11)), BR (Equation (12)), and RMG (Equations (16), (22) and (25)) shift to the right, decreasing the carbon monoxide yield. The results of increasing the carbon monoxide yield as the temperature increases are also demonstrated via fixed-bed experiments of bio-oil reforming in blast furnace slag [35].

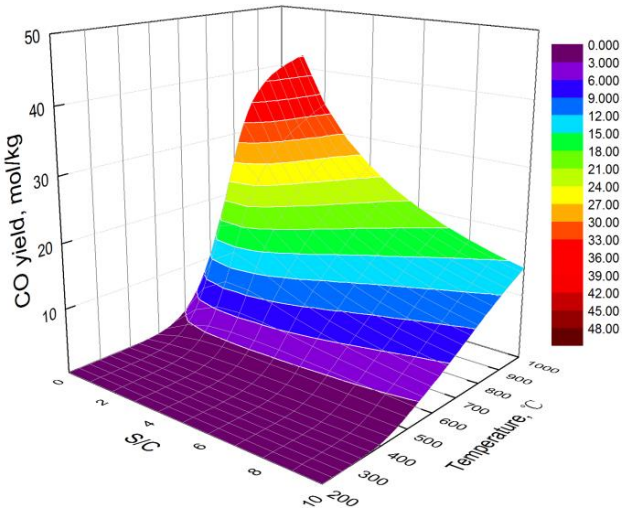

Figure 2. Carbon monoxide yields under different temperatures and S/C ratios.

Taking the characterizations of steel slag-3 as an example, the methane yields under different temperatures and S/C ratios are illustrated in Figure 3. The methane yield decreases with the increase in temperature, as shown in Figure 3. Taking S/C of 6 as an example, methane yield decreases from 24.40 mol/kg to 0.00 mol/kg as the temperature

increases from 200 °C to 1000 °C. The endothermic reactions of SRR (Equation (7)) and RMG (Equations (17), (20), (23) and (26)), and the exothermal reactions of MR (Equations (8) and (9)) are the main factors that affect the methane yield. With the increasing temperature, the endothermic reactions of SRR (Equation (7)), RMG (Equations (17), (20), (23) and (26)) shift to the right, and the exothermal reactions of MR (Equations (8) and (9)) shift to the left, decreasing the methane yield. The characterizations of hydrogen production from the steam reforming of bio-oil over a Ce-Ni/Co catalyst were investigated [41]. The results showed that the higher temperature, the lower the methane yield. These results are consistent with this study.

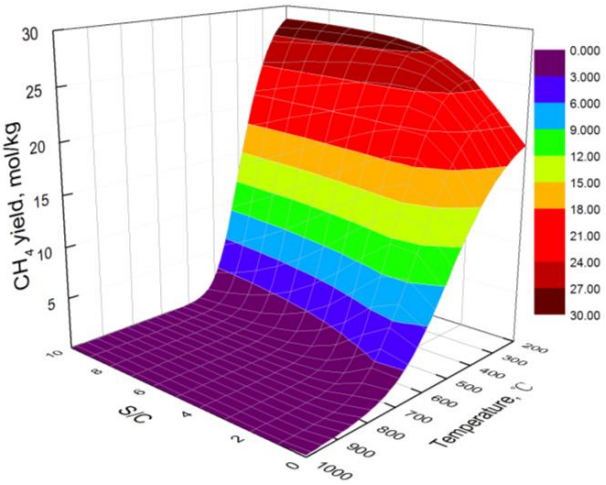

Figure 3. Methane yields under different temperatures and S/C ratios.

The process of bio-oil steam reforming using steel slag as a heat carrier generates carbon, which might decrease the reactive activation and have no benefit for the steam reaction. The carbon yield is regarded as a significant factor in the research on the steam reforming process. Taking the characterizations of steel slag-3 as an example, the carbon yields under different temperatures and S/C ratios are shown in Figure 4. As shown in Figure 4, the carbon yield decreases with the increasing temperature. Taking S/C of 5 as an example, the carbon yield decreases from 11.58 mol/kg to 0.03 mol/kg with the increase in temperature from 200 °C to 1000 °C. The endothermic reaction of WGR (Equation (10)) and the exothermal reaction of BR (Equation (12)) are the main factors that affect the carbon yield. With the increase in temperature, the endothermic reaction of WGR (Equation (10)) shifts to the right and the exothermal reaction of BR (Equation (12)) shifts to the left, decreasing the carbon yield.

Taking the characterizations of steel slag-3 as an example, the hydrogen component, carbon monoxide component, and methane component under different temperatures and S/C ratios are illustrated in Figure 5, Figure 6, and Figure 7, respectively. In Figure 5, the hydrogen component increases at the beginning and then decreases as the temperature increases. Taking S/C of 5 as an example, the hydrogen component increases from 4.95% to 70.93% with the increase in temperature from 200 °C to 608 °C, but the hydrogen component decreases from 70.93% to 67.04% with the increase in temperature from 608 °C to 1000 °C. In Figure 6, the carbon monoxide component increases with the increase in temperature. Taking S/C of 5 as an example, the carbon monoxide component increases from 0.00% to 15.42% with the increase in temperature from 200 °C to 1000 °C. In Figure 7, the methane component decreases with the increase in temperature. Taking S/C of 5 as an example, the methane component decreases from 72.24% to 0.00% with the increase in temperature from 200 °C to 1000 °C. The variations in the hydrogen component, carbon monoxide component, and methane component are attributed to their yields. Thus, the variation trends of the hydrogen component, carbon monoxide component, and methane component are similar to those of their yields.

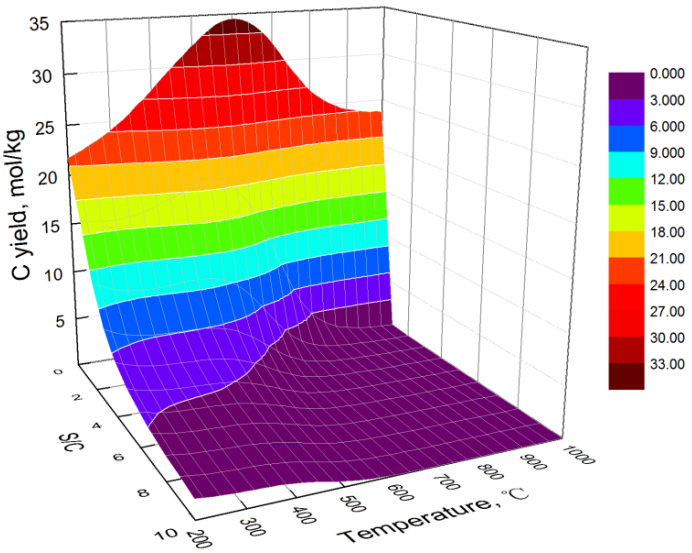

Figure 4. Carbon yields under different temperatures and S/C ratios.

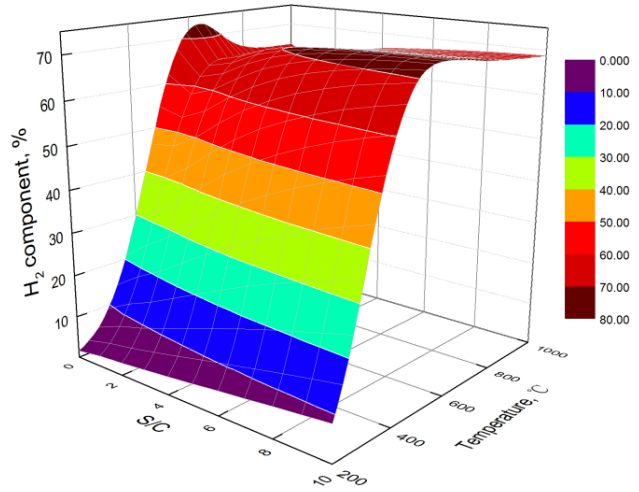

Figure 5. Hydrogen components under different temperatures and S/C ratios.

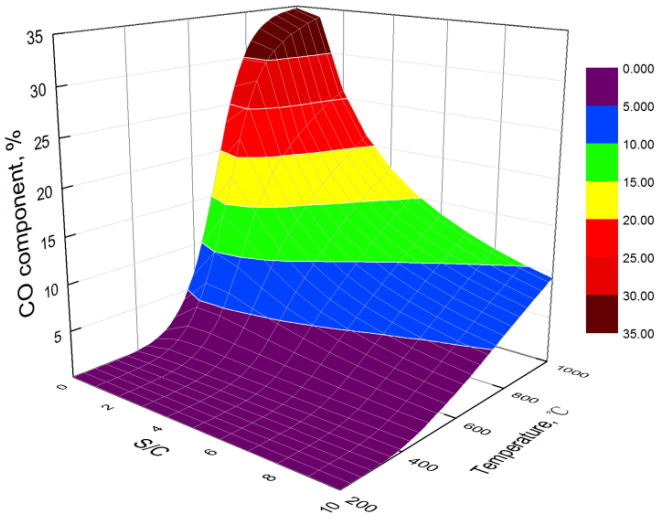

Figure 6. Carbon monoxide components under different temperatures and S/C ratios.

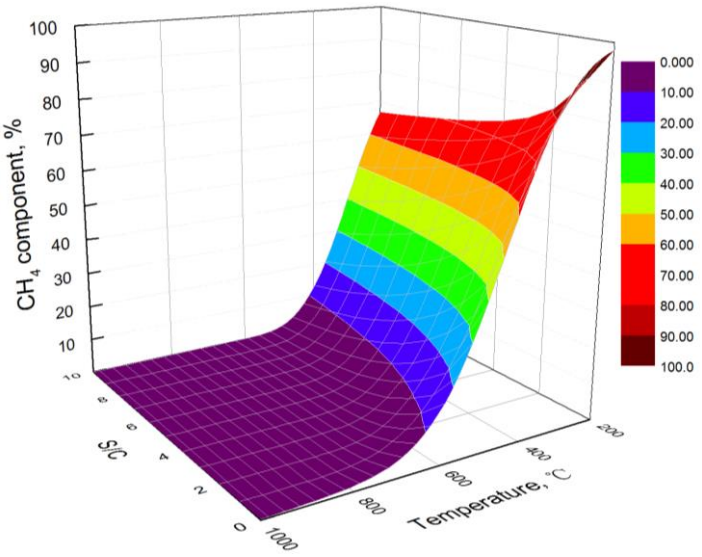

Figure 7. Methane components under different temperatures and S/C ratios.

3.2. Effect of S/C

Steam functions as the reactant during the process of steam reforming of the bio-oil recovery of waste heat from steel slag. The S/C impacts the partial pressure of steam, further affecting the equilibrium product distribution. The effects of S/C on the PY and DGC of the steam reforming of the bio-oil of recovery waste heat from steel slag are illustrated in this section.

The effects of S/C on the hydrogen yield are also shown in Figure 1. Figure 1 shows that the hydrogen yield increases with the increase in S/C. Taking the temperature of 706 °C as an example, the hydrogen yield increases from 36.08 mol/kg to 113.67 mol/kg as the S/C increases from 0 to 10. With the increase in S/C, SRR (Equations (2)–(7)), WGR (Equation (10)), and WGSR (Equation (11)) shift to the right, and MR (Equation (8)) and RMG (Equations (15), (18), (21) and (24)) shift to the left, increasing the hydrogen yield. The characterizations of bio-oil steam reforming for hydrogen production have been investigated via fixed-bed experiments [38]. The results implied that the hydrogen yield increased with the increase in S/C. These results are consistent with the findings in this study.

The effects of S/C on the carbon monoxide yield are shown in the Figure 2. Figure 2 shows that, at low temperatures (lower than 412 °C), the carbon monoxide yield increases with the increase in S/C. At low temperatures, MR (Equation (8)) and WGR (Equation (10)) are the main factors that affect the carbon monoxide yield and they shift to the left, increasing the carbon monoxide yield. However, at high temperatures (higher than 412 °C), the carbon monoxide yield increases first and then decreases with the increase in S/C. At high temperatures and low S/C, MR (Equation (8)) and WGR (Equation (10)) are the main factors that affect the carbon monoxide yield and they shift to the left, increasing the carbon monoxide yield. However, at high temperatures and high S/C, WGSR (Equation (11)) is the main factor affecting the carbon monoxide yield and it shifts to the right, decreasing the carbon monoxide yield.

The effects of S/C on the methane yield are shown in Figure 3. As shown in Figure 3, at low temperatures (lower than 216 °C), the methane yield increases with the increase in S/C. At low temperatures, RMG (Equations (17), (20), (23) and (26)) is the main factor that affects the methane yield and shifts to the left, increasing the methane yield. At high temperatures (higher than 216 °C), the methane yield increases first and then decreases with the increase in S/C. At high temperatures and low S/C, RMG (Equations (17), (20), (23) and (26)) is the main factor that affects the methane yield and shifts to the left, increasing the methane yield. However, at high temperatures and high S/C, SRR (Equation (7)) and MR (Equation (8)) are

the main factors that affect the methane yield. With the increase in S/C, SRR (Equation (7)) shifts to the right and MR (Equation (8)) shifts to the left, decreasing the methane yield.

The effects of S/C on the carbon yield are also shown in Figure 4. As shown in Figure 4, the carbon yield decreases with the increase in S/C. Taking the temperature of 690 °C as an example, the hydrogen yield increases from 32.41 mol/kg to 0.02 mol/kg with the increase in S/C from 0 to 10. WGR (Equation (7)) is the main factor that affects the carbon yield and shifts to the right with the increase in S/C, decreasing the carbon yield.

Combining the effects of temperature and S/C, when S/C is 6, the maximal hydrogen yield is 109.13 mol/kg at 706 °C. In addition, the hydrogen component and carbon yield are 70.21% and 0.08 mol/kg at 706 °C, respectively. When S/C increases to 10, the maximal hydrogen yield and hydrogen component are 115.68 mol/kg and 72.34%, respectively. The purpose of the novel technology is to utilize hydrogen to recover the waste heat of steel slag. In addition, carbon may go against the process of steam reforming of bio-oil [38,42]. The hydrogen yield and carbon yield via thermodynamic calculations are regarded as the primary indexes for evaluating the process. When S/C increases from 6 to 10, the hydrogen yield increases, although not obviously. However, the energy consumption of the process increases on account of the increasing steam [5]. The optimal temperature and S/C are 706 °C and 6, respectively, where the hydrogen yield and hydrogen component are 109.13 mol/kg and 70.21%, respectively.

3.3. Effect of Type of Steel Slag

The compositions of steel slag mainly depend on the different kinds of steelmaking processes and steel types. The iron oxides and basicity of steel slag can affect the equilibrium production of the process of the bio-oil steam reforming recovery of waste heat from steel slag. Using bio-oil steam reforming recovery of waste heat from steel slag aims to obtain hydrogen efficiently. The effects of the type of steel slag on the hydrogen yield, carbon yield, and hydrogen component are illustrated in this section. Taking S/C of 2 as an example, the hydrogen yields and hydrogen components under different types of steel slag are shown in Figures 8 and 9, respectively. As shown in Figures 8 and 9, the hydrogen yield and hydrogen component decrease with the increase in iron oxides in steel slag. Taking the temperature of 592 °C as an example, the hydrogen yield and hydrogen component decrease from 72.36 mol/kg and 65.96% to 71.79 mol/kg and 65.32%, respectively, with the iron oxides increasing from 15% to 35%. However, the hydrogen yield and hydrogen component increase with the increasing basicity of steel slag. Taking the temperature of 706 °C as an example, the hydrogen yield and hydrogen component increase from 89.85 mol/kg and 66.12% to 90.36 mol/kg and 67.53%, respectively, with the basicity increasing from 2 to 4. The basicity of steel slag is calculated via the mole ratio of CaO to SiO_2. With the increase in the basicity of steel slag, CaO in the steel slag increases accordingly. CaO absorbs carbon dioxide via RMG (Equation (11)), decreasing the carbon dioxide yield. The decreasing CO_2 yield shifts TCR (Equation (1)), SRR (Equations (2)–(7)), and WGSR (Equation (11)) to the right, increasing the hydrogen yield and hydrogen component. However, with the increase in iron oxides, CaO in the steel slag decreases accordingly, which has adverse effects on hydrogen production. In addition, with the increase in iron oxides, RMG (Equations (15), (18), (21) and (24)) is the main factor that affects the methane yield and shifts to the right, decreasing the hydrogen yield and hydrogen component. Compared with CaO in steel slag, iron oxides have less effect on hydrogen production from bio-oil steam reforming in steel slag. The appropriate decrease in iron oxides and increase in basicity can be beneficial for the process of bio-oil steam reforming recovery of waste heat from steel slag in the actual application.

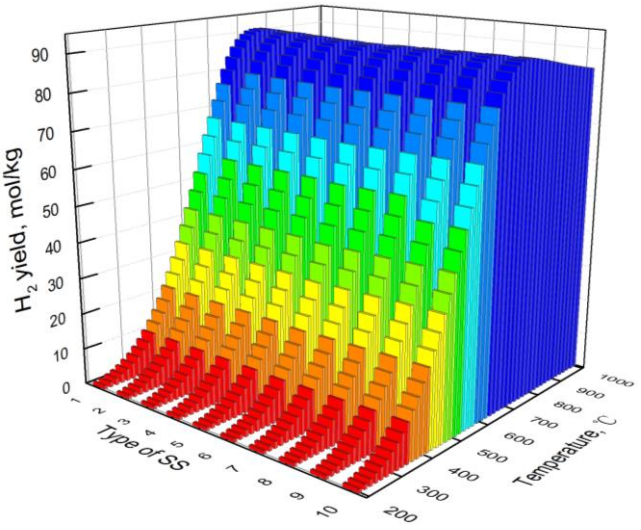

Figure 8. Hydrogen yields under different types of steel slag.

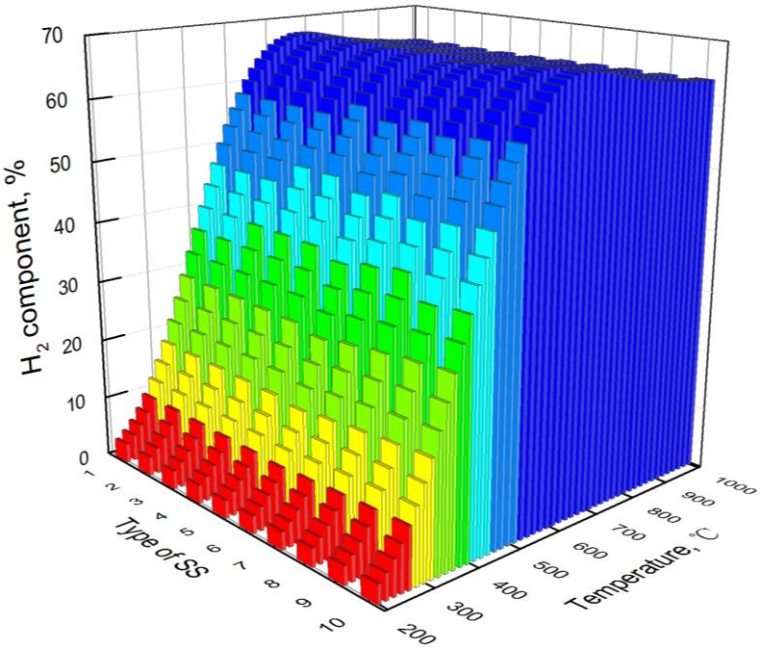

Figure 9. Hydrogen components under different types of steel slag.

3.4. The Mechanism of Recovering Waste Heat from Steel Slag

Based on the equilibrium productions and our previous studies of the chemical reactions in the recovery of waste heat from slag [2,35,36], the mechanism of bio-oil steam reforming in steel slag was obtained, as shown in Figure 10. In the practical process, steel slag is discharged via the process of steelmaking and it is shown in the slag storage pot. Bio-oil and steam in a certain proportion are fed into the slag storage pot via pipelines. The reactions of bio-oil steam reforming in steel slag take place. The syngas (containing H_2, CO, CO_2, and CH_4) is obtained and discharged from the slag storage pot. The transfer of heat due to the chemical reaction of bio-oil steam reforming and steel slag is accomplished. As shown in Figure 10, the ions of Ca^{2+}, Fe^{2+}, and Fe^{3+} in steel slag weaken the bonds of C–C and H–O [2,35,43,44], catalyzing the process of bio-oil steam reforming recovery of waste heat from steel slag. Utilization of bio-oil steam reforming efficiently recovers waste heat from steel slag.

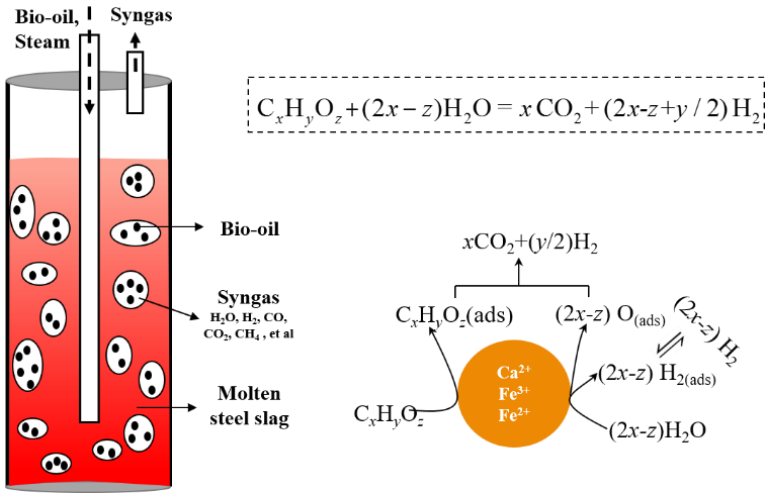

Figure 10. The mechanism of bio-oil steam reforming recovery of waste heat from steel slag.

4. Conclusions

The novel technology of the bio-oil steam reforming recovery of waste heat from steel slag was investigated via thermodynamic calculations. The primary remarks are summarized as follows:

1. The novel method of utilizing bio-oil steam reforming to recover waste heat from steel slag is proposed in this study. It is proven that bio-oil steam reforming can be used to obtain hydrogen and utilize the waste heat of steel slag, and can provide an opportunity for green metallurgy technology.
2. At low temperatures, the hydrogen yield of bio-oil steam reforming in steel slag increases with the increase in temperature. However, at high temperatures, the water gas shift reaction is the main reaction affecting the hydrogen yield, resulting in the decrease in the hydrogen yield with the increase in temperature. The carbon yield decreases with the increase in temperature. The hydrogen component increases first and then decreases with the increase in temperature.
3. The higher the S/C, the higher the obtained hydrogen yield and the lower the obtained carbon yield. By combining the hydrogen yield and energy consumption, the optimal S/C is 6 and the optimal temperature is 706 °C. At the optimal condition, the hydrogen yield, hydrogen component, and carbon yield are 109.13 mol/kg, 70.21%, and 0.08 mol/kg, respectively.
4. Compared with CaO in steel slag, iron oxides have less effect on hydrogen production from bio-oil steam reforming in steel slag. The basicity of steel slag promotes hydrogen production. During industrial application, the hydrogen yield and hydrogen component of bio-oil steam reforming in steel slag can be promoted via an appropriate decrease in iron oxides and increase in basicity.

Author Contributions: Methodology, Z.L., S.W. and J.W.; Writing—original draft, Z.D. and Y.L.; Writing—review & editing, Z.D., X.Y., Y.X. and C.L. All authors have read and agreed to the published version of the manuscript.

Funding: This research was funded by the National Natural Science Foundation of China (52274334), the Natural Science Foundation of Hebei (E2021209106), the Youth Scholars Promotion Plan of North China University of Science and Technology (QNTJ202205), the Talent Foundation of Tangshan (A202110039), the Science and Technology Planning Project of Tangshan (22130233H), and the Funds of Basic Scientific Research of Hebei (JQN202007). And the APC was funded by the Natural Science Foundation of Hebei (E2021209106).

Data Availability Statement: No new data were created or analyzed in this study. Data sharing is not applicable to this article.

Conflicts of Interest: The authors declare no conflict of interest.

References

1. Yao, X.; Yu, Q.; Wang, K.; Xie, H.; Qin, Q. Kinetic study on recovery heat of granulated blast-furnace slag through biomass gasification using CO_2 as gasification agent. *J. Therm. Anal. Calorim.* **2018**, *131*, 1313–1321. [CrossRef]
2. Yao, X.; Yu, Q.; Han, Z.; Xie, H.; Duan, W.; Qin, Q. Kinetic and experimental characterizations of biomass pyrolysis in granulated blast furnace slag. *Int. J. Hydrogen Energy* **2018**, *43*, 9246–9253. [CrossRef]
3. Available online: https://worldsteel.org/steel-topics/statistics/world-steel-in-figures-2022/ (accessed on 2 April 2023).
4. Lin, B.; Wu, R. Designing energy policy based on dynamic change in energy and carbon dioxide emission performance of China's iron and steel industry. *J. Clean. Prod.* **2020**, *256*, 120412. [CrossRef]
5. Yao, X.; Liu, Y.; Yu, Q.; Wang, S. Energy consumption of two-stage system of biomass pyrolysis and bio-oil reforming to recover waste heat from granulated BF slag. *Energy* **2023**, *273*, 127204. [CrossRef]
6. Wang, R.Q.; Jiang, L.; Wang, Y.D.; Roskilly, A.P. Energy saving technologies and mass-thermal network optimization for decarbonized iron and steel industry: A review. *J. Clean. Prod.* **2020**, *274*, 122997. [CrossRef]
7. Sun, Y.; Seetharaman, S.; Zhang, Z. Integrating biomass pyrolysis with waste heat recovery from hot slags via extending the C-loops: Product yields and roles of slags. *Energy* **2018**, *149*, 792–803. [CrossRef]
8. Sun, Y.; Zhang, Z.; Liu, L.; Wang, X. Integration of biomass/steam gasification with heat recovery from hot slags: Thermodynamic characteristics. *Int. J. Hydrogen Energy* **2016**, *41*, 5916–5926. [CrossRef]
9. Sun, Y.; Zhang, Z. Disposal of High-Temperature Slags: A Review of Integration of Heat Recovery and Material Recycling. *Metall. Mater. Trans. E* **2016**, *3*, 114–122. [CrossRef]
10. Li, P. Thermodynamic analysis of waste heat recovery of molten blast furnace slag. *Int. J. Hydrogen Energy* **2017**, *42*, 9688–9695. [CrossRef]
11. Sun, Y.; Zhang, Z.; Liu, L.; Wang, X. Heat Recovery from High Temperature Slags: A Review of Chemical Methods. *Energies* **2015**, *8*, 1917–1935. [CrossRef]
12. Yao, X.; Yu, Q.; Xie, H.; Duan, W.; Han, Z.; Liu, S.; Qin, Q. Syngas production through biomass/CO_2 gasification using granulated blast furnace slag as heat carrier. *J. Renew. Sustain. Energy* **2017**, *9*, 053101. [CrossRef]
13. Yao, X.; Yu, Q.; Wang, K.; Xie, H.; Qin, Q. Kinetic characterizations of biomass char CO_2-gasification reaction within granulated blast furnace slag. *Int. J. Hydrogen Energy* **2017**, *42*, 20520–20528. [CrossRef]
14. Kasai, E.; Kitajima, T.; Akiyama, T.; Yagi, J.; Saito, F. Rate of methane-steam reforming reaction on the surface of molten BF slag—For heat recovery from molten slag by using a chemical reaction. *ISIJ Int.* **1997**, *37*, 1031–1036. [CrossRef]
15. Duan, W.; Yu, Q.; Xie, H.; Liu, J.; Wang, K.; Qin, Q.; Han, Z. Thermodynamic analysis of synergistic coal gasification using blast furnace slag as heat carrier. *Int. J. Hydrogen Energy* **2016**, *41*, 1502–1512.
16. Duan, W.; Yu, Q.; Xie, H.; Qin, Q.; Zuo, Z. Thermodynamic analysis of hydrogen-rich gas generation from coal/steam gasification using blast furnace slag as heat carrier. *Int. J. Hydrogen Energy* **2014**, *39*, 11611–11619. [CrossRef]
17. Yao, X.; Yu, Q.; Xie, H.; Duan, W.; Han, Z.; Liu, S.; Qin, Q. The production of hydrogen through steam reforming of bio-oil model compounds recovering waste heat from blast furnace slag. *J. Therm. Anal. Calorim.* **2018**, *131*, 2951–2962. [CrossRef]
18. Li, P.; Yu, Q.; Xie, H.; Qin, Q.; Wang, K. CO_2 gasification rate analysis of Datong coal using slag granules as heat carrier for heat recovery from blast furnace slag by using a chemical reaction. *Energy Fuels* **2013**, *27*, 4810–4817. [CrossRef]
19. Li, P.; Yu, Q.; Qin, Q.; Lei, W. Kinetics of CO_2/coal gasification in molten blast furnace slag. *Ind. Eng. Chem. Res.* **2012**, *51*, 15872–15883. [CrossRef]
20. Yao, X.; Yu, Q.; Han, Z.; Xie, H.; Duan, W.; Qin, Q. Kinetics of CO_2 gasification of biomass char in granulated blast furnace slag. *Int. J. Hydrogen Energy* **2018**, *43*, 12002–12012. [CrossRef]
21. Sun, Y.; Zhang, Z.; Liu, L.; Wang, X. Two-stage high temperature sludge gasification using the waste heat from hot blast furnace slags. *Bioresour. Technol.* **2015**, *198*, 364–371. [CrossRef]
22. Sun, Y.; Zhang, Z.; Liu, L.; Wang, X. Integrated carbon dioxide/sludge gasification using waste heat from hot slags: Syngas production and sulfur dioxide fixation. *Bioresour. Technol.* **2015**, *181*, 174–182. [CrossRef] [PubMed]
23. Purwanto, H.; Akiyama, T. Hydrogen production from biogas using hot slag. *Int. J. Hydrogen Energy* **2006**, *31*, 491–495. [CrossRef]
24. Zhao, L.; Wang, H.; Qing, S.; Liu, H. Characteristics of gaseous product from municipal solid waste gasification with hot blast furnace slag. *J. Nat. Gas Chem.* **2010**, *19*, 403–408. [CrossRef]
25. Duan, W.; Yu, Q.; Liu, J.; Wu, T.; Yang, F.; Qin, Q. Experimental and kinetic study of steam gasification of low-rank coal in molten blast furnace slag. *Energy* **2016**, *111*, 859–868. [CrossRef]
26. Duan, W.; Yu, Q.; Wu, T.; Yang, F.; Qin, Q. Experimental study on steam gasification of coal using molten blast furnace slag as heat carrier for producing hydrogen-enriched syngas. *Energy Convers. Manag.* **2016**, *117*, 513–519. [CrossRef]
27. Luo, S.; Guo, J.; Feng, Y. Hydrogen-rich gas production from pyrolysis of wet sludge in situ steam agent. *Int. J. Hydrogen Energy* **2017**, *42*, 18309–18314. [CrossRef]
28. Luo, S.; Fu, J.; Zhou, Y.; Yi, C. The production of hydrogen-rich gas by catalytic pyrolysis of biomass using waste heat from blast-furnace slag. *Renew. Energy* **2017**, *101*, 1030–1036. [CrossRef]
29. Wang, P.; Xie, H.; Zhang, J.; Jia, L.; Yu, Z.; Li, R. Optimization of two bio-oil steam reforming processes for hydrogen production based on thermodynamic analysis. *Int. J. Hydrogen Energy* **2022**, *47*, 9853–9863. [CrossRef]

30. Jin, K.; Ji, D.; Xie, Q.; Nie, Y.; Yu, F.; Ji, J. Hydrogen production from steam gasification of tableted biomass in molten eutectic carbonates. *Int. J. Hydrogen Energy* **2019**, *44*, 22919–22925. [CrossRef]
31. Krzywanski, J.; Fan, H.; Feng, Y.; Shaikh, A.; Fang, M.; Wang, Q. Genetic algorithms and neural networks in optimization of sorbent enhanced H_2 production in FB and CFB gasifiers. *Energy Convers. Manag.* **2018**, *171*, 1651–1661. [CrossRef]
32. Bizkarra, K.; Bermudez, J.; Arcelus-Arrillaga, P.; Barrio, V.L.; Cambra, J.; Millan, M. Nickel based monometallic and bimetallic catalysts for synthetic and real bio-oil steam reforming. *Int. J. Hydrogen Energy* **2018**, *46*, 11706–11718. [CrossRef]
33. Valle, B.; Aramburu, B.; Benito, P.; Bilbao, J.; Gayubo, A.G. Biomass to hydrogen-rich gas via steam reforming of raw bio-oil over Ni/La_2O_3-αAl_2O_3 catalyst: Effect of space-time and steam-to-carbon ratio. *Fuel* **2018**, *216*, 445–455. [CrossRef]
34. Rodrigues, C.; Alonso, C.; Machado, G.; de Souza, T. Optimization of bio-oil steam reforming process by thermodynamic analysis. *Int. J. Hydrogen Energy* **2020**, *45*, 28350–28360. [CrossRef]
35. Yao, X.; Yu, Q.; Xu, G.; Han, Z.; Qin, Q. Production of syngas from dry reforming of bio-oil model compound in granulated blast furnace slag. *Korean J. Chem. Eng.* **2019**, *36*, 722–728. [CrossRef]
36. Yao, X.; Yu, Q.; Xu, G.; Han, Z.; Xie, H.; Duan, W.; Qin, Q. The characteristics of syngas production from bio-oil dry reforming utilizing the waste heat of granulated blast furnace slag. *Int. J. Hydrogen Energy* **2018**, *43*, 22108–22115. [CrossRef]
37. Shimada, T.; Kochura, V.; Akiyama, T.; Kasai, E.; Yagi, J. Effects of slag compositions on the rate of methane–steam reaction. *ISIJ Int.* **2000**, *41*, 111–115. [CrossRef]
38. Xie, H.; Yu, Q.; Zuo, Z.; Han, Z.; Yao, X.; Qin, Q. Hydrogen production via sorption-enhanced catalytic steam reforming of bio-oil. *Int. J. Hydrogen Energy* **2016**, *41*, 2345–2353. [CrossRef]
39. Zuo, Z.; Yu, Q.; Xie, H.; Yang, F.; Qin, Q. Thermodynamic analysis of reduction in copper slag by biomass molding compound based on phase equilibrium calculating model. *J. Therm. Anal. Calorim.* **2018**, *132*, 1277–1289. [CrossRef]
40. Xie, H.; Yu, Q.; Zhang, Y.; Zhang, J.; Liu, J.; Qin, Q. New process for hydrogen production from raw coke oven gas via sorption-enhanced steam reforming: Thermodynamic analysis. *Int. J. Hydrogen Energy* **2017**, *42*, 2914–2923. [CrossRef]
41. Xie, H.; Yu, Q.; Wei, M.; Duan, W.; Yao, X.; Qin, Q.; Zuo, Z. Hydrogen production from steam reforming of simulated bio-oil over Ce–Ni/Co catalyst with in continuous CO_2 capture. *Int. J. Hydrogen Energy* **2015**, *40*, 1420–1428. [CrossRef]
42. Xie, H.; Zhang, J.; Yu, Q.; Zuo, Z.; Liu, J.; Qin, Q. Study on Steam Reforming of Tar in Hot Coke Oven Gas for Hydrogen Production. *Energy Fuels* **2016**, *30*, 2336–2344. [CrossRef]
43. Luo, S.; Feng, Y. The production of fuel oil and combustible gas by catalytic pyrolysis of waste tire using waste heat of blast-furnace slag. *Energy Convers. Manag.* **2017**, *136*, 27–35. [CrossRef]
44. Huang, B.-S.; Chen, H.-Y.; Chuang, K.-H.; Yang, R.-X.; Wey, M.-Y. Hydrogen production by biomass gasification in a fluidized-bed reactor promoted by an Fe/CaO catalyst. *Int. J. Hydrogen Energy* **2012**, *37*, 6511–6518. [CrossRef]